Demonstration of a Conduction Cooled React and Wind MgB_2 Coil Segment for MRI Applications

H. S. Kim, C. Kovacs, M. Rindfleisch, J. Yue, D. Doll, M. Tomsic, M. D. Sumption, and E. W. Collings

Abstract—This study is a contribution to the development of technology for an MgB_2-based, cryogen-free, superconducting magnet for an MRI system. Specifically, we aim to demonstrate that a react and wind coil can be made using high performance in-situ route MgB_2 conductor, and that the conductor could be operated in conduction mode with low levels of temperature gradient. In this work, an MgB_2 conductor was used for the winding of a sub-size, MRI-like coil segment. The MgB_2 coil was wound on a 457 mm ID 101 OFE copper former using a react-and-wind approach. The total length of conductor used was 330 m. The coil was epoxy impregnated and then instrumented for low temperature testing. After the initial cool down (conduction cooling) the coil I_c was measured as a function of temperature (15-30 K), and an I_c of 200 A at 15 K was measured.

***Index Terms*—MgB_2 coil, conduction cooling, Magnet, MRI**

I. Introduction

MRI systems based on coils wound with MgB_2 are of significant interest as one way to develop liquid-cryogen-free MRI systems. MgB_2's T_c of 39 K invites conduction cooling, and its lower cost as compared to HTSC makes it an economically viable candidate. The low-T_c-like coherence length allows for persistent joints, and the intermediate T_c increases the minimum quench energy while not suppressing the normal zone velocity to the extent seen for HTSC conductors. Conductor performance is at the level needed for MRI application, and conductor designs appropriate for MRIs can be made.

A number of efforts in coil development, and specifically MRI coil development, are underway [1,2]. We have previously described a variety of coils and coil applications for MgB_2 [3-5]. However, there are several elements that need development and de-risking if conduction cooled MRI is to be developed using MgB_2. Here we focus on the winding of a coil segment and its testing via conduction cooling, focusing on the coil technology and conduction cooling aspects. MgB_2-based MRIs may be constructed either in wind and react or react and wind mode, given the respectable strain tolerance of MgB_2 and the geometry of the coil segments. A wind and react coil process simplifies initial development, but a react and wind process has several important advantages, including simpler insulation, compatibility with existing coil winding and MRI manufacturing, and dimensional control of the coil. Therefore, we have chosen to explore the react and wind approach. We do not in this case fabricate a full size MRI coil segment. For our present purposes, it is sufficient to make a sub-size coil. The main considerations in the coil design was to wind a coil pack of sufficient size to use relevant heat treatment, insulation, epoxy, and, and winding schemes to be MRI-coil relevant, as well as using a former which could achieve sufficiently small temperature gradients.

In this original work (not previously reported), an MgB_2 conductor has been used for the winding of a (sub-size) MRI-like coil segment. The purpose of the work was to demonstrate that a react and wind coil could be made using high performance in-situ route MgB_2 conductor, and that the conductor could be operated in conduction mode with low levels of temperature gradient. A key aspect of this is high quality current-transitions, a target area of this work. In order to fabricate the coil, pre-reacted, insulated MgB_2 was used, and the winding process kept winding strain on the wire to 0.1%. The coil was epoxy impregnated, and then instrumented for low temperature testing. After initial an cool down the coil I_c was measured as a function of temperature, as well as the temperature distribution within the coil.

II. Experimental

A. Conductor

The coil was wound with an in-situ route, multifilamentary MgB_2 conductor fabricated by Hyper Tech Research Inc. The conductor (strand 3364) was 0.84 mm OD, and had 36 filaments, Fig. 1. The individual Mg+B powder mixture was surrounded by a Nb chemical barrier, and the outer sheath was Monel. The interfilamentary matrix was pure Cu, as was the central filament. The starting powders consisted of Mg (99.9%, 20–25 μm) and the pre-doped B (SMI-C-doped). This wire was processed as described in [6-8]. This wire was chosen because it is a standard (typical) wire available from Hyper Tech and it has good I_c properties.

Manuscript received October 18, 2015. This work was supported by the NIH, National Institute of Biomedical Imaging and Bioengineering, under R01EB018363, and also under an NIH Bridge Grant.

H. S. Kim, M. D. Sumption, C. Kovacs, and E. W. Collings are with Center for Superconducting and Magnetic Materials, the Department of Materials Science and Engineering, The Ohio State University, Columbus, OH 43210 USA (corresponding author: H.S. Kim; phone: +1(614) 906-4812; fax: 630-840-9999; e-mail: kim.3237@osu.edu.).

M Rindfleisch, J Yue, D. Doll, and M. Tomsic are with Hyper Tech Research Incorporated, 539 Industrial Mile Road, Columbus, Ohio 43228, USA.

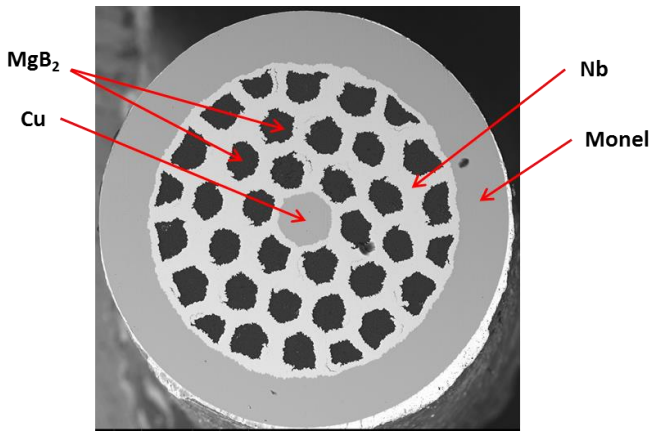

Fig. 1. Scanning Electron Microscope (SEM) image of MgB_2 conductor cross section, shown at a wire OD of 0.84 mm.

The conductor was heat treated at 675°C for 90 minutes under Argon prior to coil winding. Further details of the strand are given in Table I.

TABLE I:WIRE SPECIFICATION FOR STRAND 3364

Barrier	Mono/Multi sheath	Central fil(s)	powder material	dia (mm)	% powder
Nb	Cu/Monel	Cu	MgB_2,2%C	0.84	18.1

B. *Coil Winding and Epoxy Impregnation*

The MgB_2 coil was wound on a 457 mm ID 101 OFE copper former using the react-and-wind method. The conductor was s-glass insulated and had a total length of 332 m. The coil was vacuum impregnated with CTD epoxy. Further coil specifications are given in Table II.

TABLE II: SPECIFICATIONS OF THE COIL

OD [mm]	ID [mm]	Height [mm]	cross sectional area [mm^2]	No. Turns	Total conduct [m]	No. Layers
482.2	457.2	19.69	246.1	225	332	12

C. *Instrumentation*

After coil winding and epoxy impregnation (performed at Hyper Tech Research), the coil was delivered to OSU, where it was instrumented with voltage taps and temperature sensors. The basic layout of the voltage taps is presented linearly in Fig. 2. Here the coil is imagined to be "unravelled", and the positions of the voltage taps are shown, starting at the left with the current injection lug at its associated voltage tap, V_{CTI}, and finishing at the current out lead. Table III lists the lenghts and resistances of the various segments at room temperature.

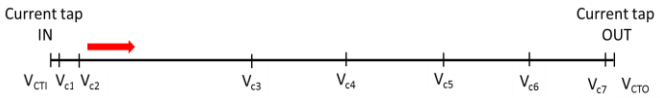

Fig. 2. Schematic voltage tap layout of the coil, with relative tap spacings shown.

In order to place the voltage taps within the winding, we used an access window which had been placed in the former, on the top of the coil directly above the winding. This access window was sealed during winding and subsequent epoxy impregnation. This sealing was removed after epoxy impregnation, the wire insulation and epoxy layer carefully removed, and solder connections were then made for the voltage taps. The instrumented coil is shown in Fig. 3, where the window can be seen in one of the insets.

TABLE III: VOLTAGE TAP LISTING, RESISTANCE, AND LENGTH

Voltage taps	Resistance @ RT [Ω]	Estimated length [cm]
CTI – C1	0.00249	1.94
C1 – C2	0.135	105.6
C2 – C3	13.9	10849
C3 – C4	7.07	5522
C4 – C5	7.12	5559
C5 – C6	7.08	5526
C6 –C7	6.81	5313
C7 – CTO	0.00478	3.73

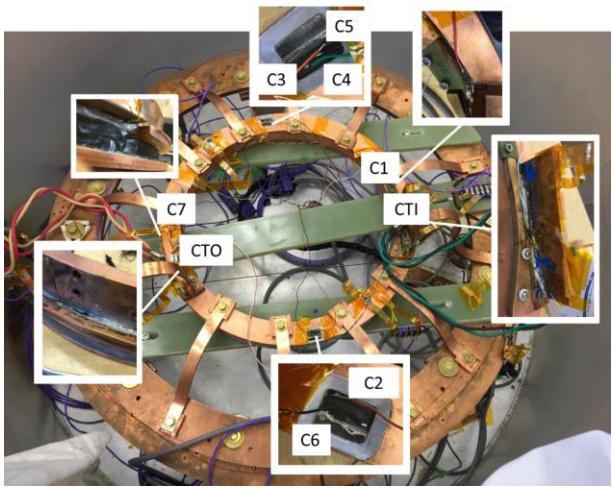

Fig. 3. The coil as positioned inside dewar, mounted to coil ring via cooling straps, with voltage instrumentation shown. Details of voltage tap connections are shown in insets.

The coil was also intrumented with cernox and E-type thermocouple temperature sensors. Table IV gives the type and position of each temperature sensor, and Fig. 4 shows their placement on the coil. Also shown in Fig. 4 are the Cu straps which connect the coil thermally to the Cu ring. There are 12 of these Cu strap connections: 10 for the coil proper, and 2 directly mounted onto the Current injection lugs. Each Cu strap is in fact a set of thin Cu straps. They are mounted to the two rings with bolts and washers, with N-grease at the interface. The bolts are tightened using a torque wrench.

III. RESULTS AND DISCUSSION

A. *Cooling Down*

After fabrication and instrumentation, the coil was inserted into OSU's general-purpose, large cryocooled test dewar, Fig. 5. This system can take coils up to 0.9 m in diameter and 0.5 m high. The cryostat uses two Sumitomo CSW-71

TABLE IV
TEMPERATURE SENSOR TYPE, NAME, AND PLACEMENT

Sensors	Location/Description
CTI 1	1st Type-E Thermocouple on "IN" current tap
CTI 2	2nd Type-E Thermocouple on "IN" current tap
CTO 1	1st Type-E Thermocouple on "OUT" current tap
CTO 2	2nd Type-E Thermocouple on "OUT" current tap
C1	1st Type-E Thermocouple on the top surface of coil
C2	2nd Type-E Thermocouple on the top surface of coil
CS	Type-E Thermocouple on the side surface of coil
CL1	1st Type-E Thermocouple on BSCCO current lead
CL2	2nd Type-E Thermocouple on BSCCO current lead
C1_cernox	CERNOX sensor on the top surface of coil
CR_cernox	CERNOX sensor on the top surface of cold ring
CTI_cernox	CERNOX sensor on "IN" current tap
CTO_cernox	CERNOX sensor on "OUT" current tap

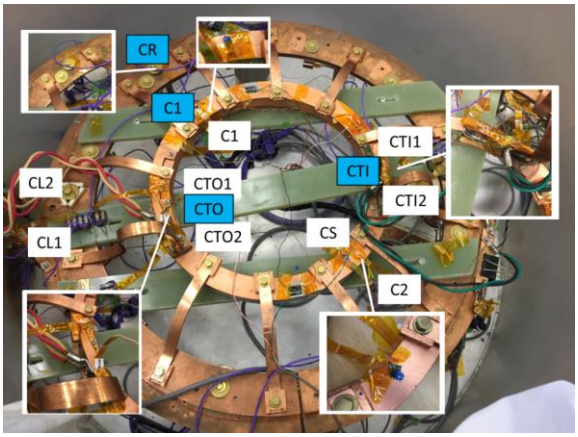

Fig. 4. Coil as positioned inside dewar, mounted to coil ring via cooling straps, with temperature instrumentation shown. Details of the temperature sensor connections are shown in insets.

compressors each mated to a Sumitomo 415D cold-head (1.5 W cooling power from each cold-head at 4.2 K) mounted to the bottom of the cooling ring shown in Fig. 4 above. The current is brought in through the thermal shield (an inner Al can) using Bi:2223 current leads.

After putting the system under vacuum, the cryocoolers were turned on and the cool-down of the system was recorded as shown in Fig. 6. The system was initially set for a target temperature of 20 K, which was reached within 24 h. During cooldown, a DC current of 10 mA was applied to the current injection lugs (CTI-1,2) and the voltage was measured on all voltage taps. This allowed us to measure the coil resistance during cool- down, as shown in Fig. 7. Here a sudden voltage drop at t = 22.08 h corresponds to a superconducting transition at 34 K. Different voltages on different segments represent different lengths between the voltage taps. The T_c of 34 K is consistent with the C-doping which this strand has (see Table I), well-known to reduce T_c from its nominal value of 39 K.

B. Critical current measurement

Once the coil temperature equilibrated at 20 K for one day (to allow the superconducting current leads to reach sufficiently low temperature for operation) a series of I_c measurements were initiated.

Fig. 5. OSU's Large cryocooler. Coils up to 0.9 m OD and 0.5 m high can be measured at temperatures down to 4 K.

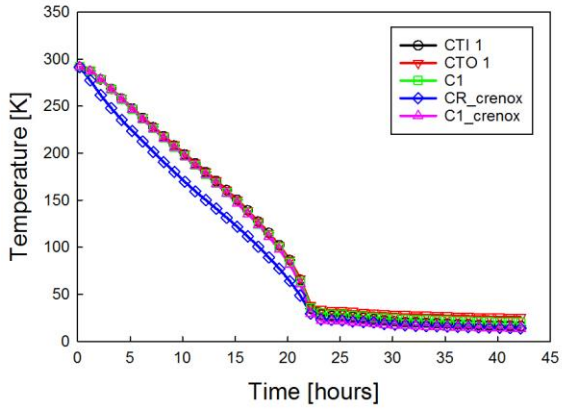

Fig. 6. Cool down of the coil from room temperature. The coil reached 20 K within 24 hours.

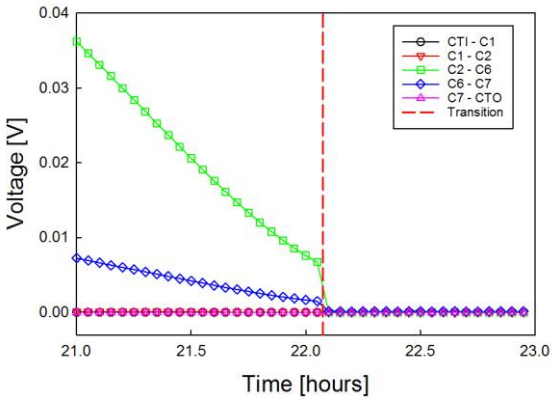

Fig. 7. Voltage across various segments of the coil with 10 mA applied to the whole coil. Measurement is shown as a function of time. A sudden resistivity drop shown at t = 22.08 h is seen for all segments (T = 34 K), and represents the superconducting transition.

The system was cooled down to 15 K, and then the I_c of the coil was measured at various temperatures ranging from 15-30 K, at current ramping rates of from 0.1 A/s to 5 A/s. No field except the coil's own field was present. A superconducting criterion of 1 μV/cm was set, however, the transition were typically by quench. Fig. 8 shows a typical set of curves, in this case at 20 K, using a current ramp rate of 2 A/s. We can

see some heating at the current taps, due to I^2R losses at the solder connections near the current injection site. The temperature increase was larger for slower ramps (e.g., 0.1 A/s) and less for higher ramp rates (5 A/s). Table V shows the *I-V* measurements performed at different nominal temperatures and ramp rates. The I_c values obtained are shown, as well as the temperature on the coil former and on the current tap at the beginning of the run as well as at its end. These results are summarized in Fig. 9 where coil I_c is shown as a function of temperature with different curves for the different ramp rates. A load line analysis has not yet been performed, but the 15 K I_c is consistent with results on similar strands. One of the key aspects of the present work was to test the quality of the end transitions, which did not allow us to preferentially cool them. Thus some current tap heating was seen at lower temperatures (where currents were higher) and for slower magnet current ramps. However, we could observe that the coil, as well as the performance of the current junctions, was good. The coil transitioned by quench, and no resistive baseline was seen.

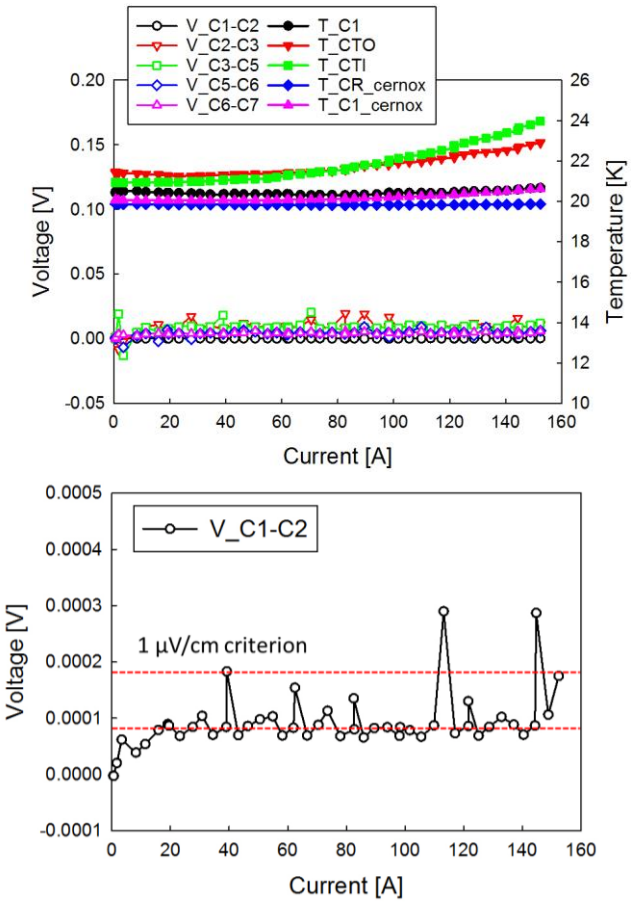

Fig. 8. (top) *I-V* curves at 20 K using a current ramping rate of 2 A/s, (bottom) expanded view of I-V curve for taps Vc1-VC2 showing that below the quench, the 1 μV/cm criterion was not exceeded, allowing an I_c to be defined. The lower dotted line gives the baseline (non-zero because of the inductive component of the coil), and the upper dotted line shows the definition of I_c (the doted lines are separated by 1 μV/cm).

TABLE V
SUMMARY OF CRITICAL CURRENT MEASUREMENTS OF COILS

Temp	Rate (A/s)	I_c (A)	Temp @ Coil (ΔT) (K)	Temp @ Current Tap IN (ΔT) (K)
30 K	2	**23.3**	29.4 ~ 29.4 (0.0)	29.9 ~29.9 (0.0)
	0.1	17.6	29.6 ~ 9.9 (0.3)	30.1 ~ 30.4 (0.3)
27 K	2	**50.5**	27.1 ~ 27.1 (0)	27.3 ~ 27.4 (0.1)
	0.1	50.1	27.1 ~ 27.1 (0)	27.3 ~ 27.8 (0.5)
22.5 K	5	116	22.5 ~ 22.7 (0.2)	23.0 ~ 24.0 (1.0)
	2	**116.5**	22.6 ~ 22.8 (0.2)	22.6 ~ 24.2 (1.6)
	0.1	111.7	22.5 ~ 23.1 (0.6)	22.9 ~ 25.3 (2.4)
20 K	5	152.4	20.0 ~ 20.5 (0.5)	20.6 ~ 23.1 (2.5)
	2	**152.4**	20.1 ~ 20.6 (0.5)	21.0 ~ 24.0 (3)
	0.1	140.6	20.1 ~ 21.4 (1.3)	20.5 ~ 24.2 (3.7)
17 K	5	187.0	17.1 ~ 18.1 (1.0)	18.0 ~22.3 (4.3)
	2	**183.8**	17.4 ~ 18.6 (1.2)	16.7 ~ 22.6 (5.9)
	0.1	173.6	17.2 ~ 18.9 (1.7)	16.9 ~ 23.3 (6.4)
15 K	5	204.6	15.1 ~ 16.8 (1.7)	16.6 ~ 22.7 (6.1)
	2	**196.7**	15.1 ~ 17.2 (2.1)	16.6 ~ 23.5 (6.9)
	0.1	191.7	15.1 ~ 17.2 (2.1)	16.5 ~ 23.5 (7.0)

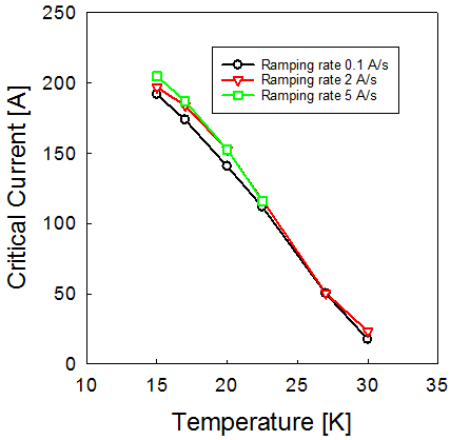

Fig. 9. Critical currents of coil as a function of temperature and ramping rate.

IV. SUMMARY

An MgB_2-based react and wind coil was made and tested as part of a technology development effort for MgB_2-based, cryogen-free, MRI. A 36 filament MgB_2 conductor was used to wind a small MRI-segment-like coil using a react and wind protocol. The coil was 457 mm ID and used a conductor length of 330 m. The coil was then epoxy impregnated, instrumented, and tested. The coil I_c was measured as a function of temperature. Modest current tap heating was seen at lower temperatures (where currents were higher) and for slower magnet current ramps. This was due to the fact that no sub-cooling of the current injection regions was used, because to do so would not allow us to test the quality of the current taps. Both the coil itself and the terminations were seen to perform well. The coil transitioned by quench, and no resistive baseline was seen. A coil I_c of 200 A was seen at 15 K.

REFERENCES

[1] W. Yao , J. Bascunan , W.-S. Kim , S. Hahn , H. Lee and Y. Iwasa "A Solid Nitrogen Cooled MgB_2 Demonstration Coil for MRI Applications", IEEE Trans. Appl. Supercond., **18** 912-915 (2008).

[2] S. Mine, M. Xu, S. Buresh, W. Stautner, C. Immer, E.T. Laskaris, K. Amm, G. Grasso, "Second Test Coil for the Development of a Compact 3 T MgB_2 Magnet", IEEE Trans Supercond. **23** 4601404 (2012).

[3] M.D. Sumption, M. Bhatia, F. Buta, S. Bohnenstiehl, M. Tomsic, M. Rindfleisch, J. Yue, J. Phillips, S. Kawabata, and E.W. Collings, "Multifilamentary MgB_2-Based Solenoidal and Racetrack Coils", Physica C **458** 12-20 (2007).

[4] M.D. Sumption, M. Bhatia, M. Rindfleisch, J. Phillips, M. Tomsic, and E. W. Collings "MgB_2/Cu Racetrack Coil Winding, Insulating, and Testing", IEEE Trans. Appl. Supercond. **15** 1457-1460 (2005).

[5] M.D. Sumption, S.A. Bohnenstiehl, F. Buta, M. Majoros, S. Kawabata, M. Tomsic, M. Rindfleisch, J. Phillips, J. Yue, and E.W. Collings, "Wind and React and React and Wind MgB_2 Solenoid, Race Track and Pancake Coils", IEEE Trans. Appl. Supercond. **17** 2286-2290 (2007).

[6] G. Z. Li, K. M. Reddy, J. B. Zwayer, M. A. Kuldell, M. A. Susner, Y. Yang, M. D. Sumption, J. J. Yue, M. A. Rindfleisch, M. J. Tomsic, C. J. Thong, and E. W. Collings, "Critical Current Density and Current Transfer Length of Multifilamentary MgB_2 Strands of Various Design", IEEE Trans. Appl. Supercond. 23 6200204 (2013).

[7] M.A Susner, T.W. Daniels, M.D. Sumption, M.A. Rindfleisch, C.J. Thong and E.W. Collings, Drawing Induced Texture and the Evolution of Superconductive Properties with Heat Treatment Time in Powder-in-tube in-situ Processed MgB_2 Strands", Supercond. Sci. Technol. **25** 065002 (2012).

[8] Y. Yang, M.A. Susner, M.D. Sumption, M. Rindfleisch, M. Tomsic, and E.W. Collings, "Influence of Strand Design, Boron Type, and Carbon Doping Method on the Transport Properties of Powder-in-Tube $MgB_{2-x}C_x$ Strands", IEEE Trans. Appl. Supercond. **22** 6200110 (2012).